Deconfining phase transition on lattices with boundaries at low temperature

Alexei Bazavov[1,2] and Bernd A. Berg[1,2]

[1]*Department of Physics, Florida State University, Tallahassee, Florida 32306-4350, USA*

[2]*School of Computational Science, Florida State University, Tallahassee, Florida 32306-4120, USA*

(Received 16 January 2007; revised manuscript received 19 March 2007; published 12 July 2007)

In lattice gauge theory (LGT) equilibrium simulations of QCD are usually performed with periodic boundary conditions (BCs). In contrast, deconfined regions created in heavy ion collisions are bordered by the confined phase. Here we discuss BCs in LGT with respect to their suitability to model a cold exterior of the lattice volume. Subsequently, we perform Monte Carlo (MC) simulations of pure SU(3) LGT with a thus inspired simple change of BCs using volumes of a size comparable to those typically encountered in the BNL relativistic heavy ion collider (RHIC) experiment. Corrections to the usual LGT results survive in the finite volume continuum limit. We estimate them as a function of the volume size for the temporal extensions $N_\tau = 4$ and 6 of the lattice and find that the results collapse to one curve when the previously established SU(3) scaling relation for the Wilson action is used. In magnitude the corrections found are comparable to those of including quarks. As observables we use a pseudocritical temperature, which rises opposite to the effect of quarks, and the width of the transition, which broadens similar to the effect of quarks.

DOI: 10.1103/PhysRevD.76.014502 PACS numbers: 12.38.Gc, 05.10.Ln, 11.15.Ha

I. INTRODUCTION

At a sufficiently high temperature QCD is known to undergo a phase transition from our everyday phase, where quarks and gluons are confined, to a deconfined quark-gluon plasma. Since the early days of lattice gauge theory simulations of this transition have been a subject of the field [1], see [2] for reviews. Naturally, such simulations focused on boundary conditions (BCs) which are favorable for reaching the infinite volume quantum [3] continuum limit quickly. On lattices of size $N_\tau N_s^3$ these are periodic BCs in the spatial volume $V = (aN_s)^3$, where a is the lattice spacing. For a textbook, see, e.g., Ref. [4].

The physical temperature of the system on a $N_\tau N_s^3$ lattice, $N_\tau < N_s$, is given by

$$T = \frac{1}{aN_\tau} = \frac{1}{L_\tau}. \tag{1}$$

In this paper we set the physical scale by [5],

$$T^c = 174 \text{ MeV} \tag{2}$$

for the deconfinement temperature, which is approximately the average from QCD estimates with two light flavor quarks [2] in the infinite volume extrapolation. The relation (1) implies for the temporal extension of the system

$$L_\tau = aN_\tau = 1.13 \text{ fermi}. \tag{3}$$

For the deconfinement phase created in a heavy ion collision, the infinite volume limit $N_s/N_\tau \to \infty$ for fixed N_τ and subsequently $N_\tau \to \infty$ ($L_\tau = aN_\tau$ finite) does not apply. Instead we have to take the continuum limit as

$$N_s/N_\tau = \text{finite}, \qquad N_\tau \to \infty, \qquad L_\tau \text{ finite}, \tag{4}$$

and periodic BCs are incorrect because the outside is in the confined phase at low temperature. Details are discussed in the next section.

In collisions at the BNL RHIC [6] one expects to create an ensemble of differently shaped and sized volumes, which contain the deconfined quark-gluon plasma. The largest volumes are those encountered in central collisions. A rough estimate of their size is

$$\pi \times (0.6 \times \text{Au radius})^2 \times c \times (\text{expansion time}) = (55 \text{ fermi}^2) \times (\text{a few fermi}), \tag{5}$$

where c is the speed of light. In our exploratory study we are content to estimate the magnitude of corrections for pure SU(3) lattice gauge theory (LGT) in volumes of this size. We stay with N_s^3 volumes and focus on the continuum limit for

$$L_s = aN_s = (5\text{–}10) \text{ fermi}. \tag{6}$$

Finite volume corrections to the infinite volume continuum limit are expected to be relevant as long as the volume is not large compared to a typical hadronic correlation length, which is about one fermi, and for such relatively small volumes an appropriate modeling of the BCs is important.

In the next section we introduce BCs which reflect a (very) low temperature outside the deconfined region. Two constructions, the "disorder wall" and the "confinement wall" are carried out and shown to exhibit the usual asymptotic scaling properties in the finite volume continuum limit. While the confined wall is physically more accurate, the disorder wall can be easily implemented in MC calculations and is used for the simulations of pure SU(3) LGT in Sec. III. A summary and conclusions are given in Sec. IV.

II. BOUNDARY CONDITIONS

Statistical properties of a quantum system with Hamiltonian H in a continuum volume V, which is in equilibrium with a heatbath at physical temperature T, are determined by the partition function [4]

$$Z(T, V) = \mathrm{Tr} e^{-H/T} = \sum_{\phi} \langle \phi | e^{-H/T} | \phi \rangle, \tag{7}$$

where the sum extends over all possible states $|\phi\rangle$ of the system and the Boltzmann constant is set to one. Imposing periodic boundary conditions in Euclidean time τ and bounds of integration from 0 to $1/T$, one can rewrite the partition function (7) in the path integral representation:

$$Z(T, V) = \int D\phi \exp\left\{ - \int_0^{1/T} d\tau L_E(\phi, \dot{\phi}) \right\}. \tag{8}$$

Nothing in this formulation requires to carry out the infinite volume limit. On the contrary, if one deals with rather small volumes consideration of $V \to \infty$ instead of finite V appears to be rather obscure.

An obvious problem of applying equilibrium thermodynamics to deconfined volumes at RHIC is that there is no heatbath with which the system could be in equilibrium. However, arguments have been made in the literature that after the rapid heating quench, when the deconfined volume is at about its maximum size, a (pseudo)equilibrium state is reached for a transition period which is reasonably long on the scale of the relaxation times involved. These arguments are not beyond doubt (some are raised in one of our own papers [7]). Here we limit our investigation to consider difficulties and effects encountered when one equilibrates a hot volume with cold boundaries by means of MC simulations for which the updating process provides the balance, so that finite volumes can be equilibrated with various BCs imposed. For simplicity and to be definite, we restrict our discussion to pure SU(3) LGT. Generalization of the arguments of this section to full QCD appears to be straightforward.

We use the single plaquette Wilson action on a 4D hypercubic lattice. Numerical evidence suggests that for N_τ fixed and $N_s \to \infty$ SU(3) lattice gauge theory exhibits a deconfining phase transition (subscript or superscript t stands for transition) at some coupling $\beta_t^g(N_\tau) = 6/g_t^2(N_\tau)$, which is weakly first order [8]. The scaling behavior of the deconfining temperature is

$$T^c = c_T \Lambda_L, \tag{9}$$

where c_T is a dimensionless constant and we use the lambda lattice scale

$$a\Lambda_L = f_\lambda(\beta^g) = \lambda(g^2)(b_0 g^2)^{-b_1/(2b_0^2)} e^{-1/(2b_0 g^2)}, \tag{10}$$

where a is the lattice spacing. The coefficients b_0 and b_1 are perturbatively determined by the renormalization group equation and independent of the renormalization prescription [9],

$$b_0 = \frac{11}{3}\frac{3}{16\pi^2} \quad \text{and} \quad b_1 = \frac{34}{3}\left(\frac{3}{16\pi^2}\right)^2. \tag{11}$$

For perturbative and nonperturbative corrections we adopt the analysis of Boyd *et al.* [10] in the parametrization [11]:

$$\lambda(g^2) = 1 + a_1 e^{-a_2/g^2} + a_3 g^2 + a_4 g^4 \tag{12}$$

with $a_1 = 715\,537\,50$, $a_2 = 19.480\,99$, $a_3 = -0.037\,724\,73$, and $a_4 = 0.508\,905\,2$.

Let us first show that LGT thermodynamics allows not only to approach the infinite volume continuum limit, but also finite volume continuum limits. For instance, we can define the thermodynamics on a torus which has the volume of, say, (10 fermi)^3. To achieve a continuum limit, we have to send the lattice spacing $a \to 0$ in units of the physical scale. This is governed by the renormalization group equation and requires $N_s = L_s/a \to \infty$, while the physical volume of the lattice stays finite by arranging $L_s/\mathrm{fermi} = c_1$, where c_1 is a constant. The temperature of such a system is regulated by choosing $L_\tau/L_s = c_2$, where c_2 is a second constant. For describing deconfined volumes at RHIC the thus defined toroidal mini-universe is even less suitable than the conventionally used infinite volume limit, because correlations are artificially propagated through the periodic BCs.

We present now two constructions of BCs, which reflect cold exterior volumes. The second is physically more realistic, but numerically more difficult to implement. The influence of such boundaries falls off like $\exp(-x/\xi)$, where x is the distance from the closest boundary and ξ a correlation length. In the infinite volume limit the usual bulk properties are obtained, because $x \gg \xi$ holds for almost all coordinates. For volumes of sizes $L_s \sim \xi$, in which we are interested, $x \gg \xi$ coordinates do not exist, so that one ends up with a finite correction to the infinite volume bulk properties.

A. Disorder wall

Imagine an almost infinite space volume $V = L_s^3$, which may have periodic BCs, and a smaller (very large, but small compared to V) subvolume $V_0 = L_{s,0}^3$. The complement to V_0 in V will be called V_1. The number of temporal lattice links N_τ is the same for both volumes. We want to find β^g values and lattice dimensions so that scaling holds, while V_0 is at a temperature of $T_0 = 174$ MeV and V_1 at T_1, say at room temperature. We set the coupling β^g to β_0^g for plaquettes in V_0 and to β_1^g for plaquettes in V_1. For that purpose any plaquette touching a site in V_1 is considered to be in V_1. Let us take $\beta_1^g = 5.7$, which is at the beginning of the SU(3) scaling region. We have

$$10^{10} \approx \frac{T_0}{T_1} = \frac{a_1}{a_0} = \frac{f_\lambda(\beta_1^g)}{f_\lambda(\beta_0^g)}, \tag{13}$$

where a_i is the lattice spacing in V_i, $i = 0, 1$. Using (10) yields $\beta_0^g \approx 25$. T_c estimates from MC calculations of the

literature extrapolate then to $L_\tau > 10^{11}a$ for the temporal lattice extension needed for the deconfined phase. This illustrates the orders of magnitude involved.

So, in practice we can only have β_0^g, but not β_1^g in the scaling region, say $\beta_0^g = 6$. There is still a reasonable choice for β_1^g. Equation (13) shows that in lattice units a correlation length ξ, say one fermi, is at β_0^g much larger than at β_1^g:

$$\frac{(\xi/a_0)}{(\xi/a_1)} = \frac{a_1}{a_0} \approx 10^{10}. \tag{14}$$

Now ξ/a_0 is of order one at $\beta_0^g = 6$, so that ξ/a_1 becomes very small and the lowest order of the strong coupling expansion applies (see [4,12] for the string tension and [13] for the glueball mass) in which $\xi/a_1 \sim -1/\ln(\beta_1^g/18)$ so that $\beta_1^g \approx 10^{-10^{10}}$. We call this construction the disorder wall.

The disorder wall allows for a finite volume continuum limit, which is approached for $\beta_0^g \to \infty$, and the usual scaling law holds. Certainly it sets in for $\beta_0^g > 25$ on astronomically large lattices. On lattices which are accessible in practice, it is less clear whether scaling will already hold: β_0^g can be chosen in the scaling region and the ratio (14) is the desired one, but for physically small volumes we have presently no theoretical control over the question whether β_1^g in the strong coupling region will introduce corrections to scaling. Therefore, it is nontrivial that our SU(3) simulation in Sec. III supports that scaling in β_0^g holds already for β_0^g values, which can be reached in practice. However, there is still another problem with the disorder wall, which is discussed next.

B. Confinement wall

In the continuum limit the disorder wall separates regions in which a correlation length ξ takes on entirely different magnitudes when measured in units of the lattice spacing (14). Although we are only interested in the physics inside the wall, a construction for which the physical length of one spacelike lattice spacing stays constant across the boundary is desirable. Along similar lines as before, this can be achieved by using an anisotropic lattice for the volume V_1 outside of the deconfined region. Let us denote in V_1 the spacelike links by a_s, the timelike links by a_τ, and use there the Wilson action

$$S(\{U\}) = \frac{\beta_s^g}{3}\sum_{\square_s}\mathrm{Re}\,\mathrm{Tr}(U_{\square_s}) + \frac{\beta_\tau^g}{3}\sum_{\square_\tau}\mathrm{Re}\,\mathrm{Tr}(U_{\square_\tau}), \tag{15}$$

where β_s^g and β_τ^g are the couplings of the spacelike and timelike plaquettes, respectively. The lambda scale of this action has been investigated by Karsch [14] and in the continuum limit one finds [15]

$$\frac{\beta_\tau^g}{\beta_s^g} = \left(\frac{a_s}{a_\tau}\right)^2. \tag{16}$$

When we aim at $a_0 = a_s \approx 10^{-10}a_\tau$ the resulting orders of magnitude are even more astronomical than before. The sublattice V_1 is again driven out of the scaling region, which would be reached for sufficiently large values of $\beta_{\mathrm{Karsch}}^g = \sqrt{\beta_s^g\beta_\tau^g}$. For practical purposes we are again driven to $\beta_\tau^g = 0$, and the simulation of the confined world becomes effectively 3D. By measuring an appropriate correlation length, for instance via the string tension or glueball mass [16], we can nonperturbatively tune β_s^g, so that $a_s = a_0$ holds. But we do not expect that the ratio of string tension to glueball mass is the same in 3D as in 4D and the matching of the spacelike lattice spacings remains approximate as long as β_τ^g stays in the strong coupling limit.

However, once one is willing to go through the computational effort of including a real outside lattice, one may in a first step be content with a temperature slightly below the deconfining temperature on the outside. Then the confinement wall will allow to have all β-values in their scaling regions and one would expect that the thus obtained results provide lower bounds on the real corrections. In the following MC study we consider only the disorder wall with $\beta_1^g = 0$, which is computationally least demanding.

III. SU(3) MC SIMULATIONS WITH THE DISORDER WALL

We approximate a cold exterior by $\beta_1^g = 0$ on the outside lattice. In practice this means we simply omit plaquettes, which involve links through the boundary. So we drop the subscript of the β_0^g definition and return to simply using the β^g notation. For both periodic and disorder wall BCs we present an analysis of data from simulations on $N_\tau \times N_s^3$ lattices with $N_\tau = 4$ and 6. Our statistics (in sweeps) is compiled in Tables I and II together with estimates of pseudocritical coupling constant values (defined below) and the number of β values at which simulations were performed in the neighborhood of the transition point. In the following, error bars are calculated with respect to 32 jackknife bins of the entire statistics at each simulation point (see, e.g., [17] for details).

As in [10] we use the maxima of the Polyakov loop susceptibility

TABLE I. Number of measurements (N_{meas} in sweeps), number of β-patches (N_β), and pseudotransition coupling estimates $\beta_{\mathrm{pt}}^g(N_s;4)$ for $4 \times N_s^3$ lattices.

	Periodic BCs			Disorder wall BCs		
N_s	N_{meas}	N_β	$\beta_{\mathrm{pt}}^g(N_s;4)$	N_{meas}	N_β	$\beta_{\mathrm{pt}}^g(N_s;4)$
12	320 000	5	5.6904 (27)	1 280 000	18	6.110 (34)
16	320 000	3	5.6912 (11)	1 280 000	11	5.8460 (83)
20	320 000	3	5.691 84 (69)	320 000	8	5.7744 (59)
24	320 000	3	5.691 70 (41)	320 000	7	5.7426 (30)
32	320 000	3	5.692 25 (16)	320 000	4	5.7192 (11)

TABLE II. As the previous table for $6 \times N_s^3$ lattices.

	Periodic BCs			Disorder wall BCs		
N_s	N_{meas}	N_β	$\beta^g_{\text{pt}}(N_s;6)$	N_{meas}	N_β	$\beta^g_{\text{pt}}(N_s;6)$
18	320 000	6	5.8932 (48)	320 000	16	6.47 (14)
20	···	···	···	320 000	11	6.27 (04)
24	320 000	4	5.8934 (26)	320 000	16	6.089 (23)
28	···	···	···	320 000	19	6.012 (11)
32	320 000	3	5.8927 (12)	320 000	11	5.9812 (73)
40	···	···	···	320 000	6	5.9463 (53)
48	···	···	···	192 000	3	5.9271 (38)

$$\chi_{\max} = \frac{1}{N_s^3}[\langle |P|^2\rangle - \langle |P|\rangle^2]_{\max}, \qquad P = \sum_{\vec{x}} P_{\vec{x}} \tag{17}$$

to define pseudotransition couplings $\beta^g_{\text{pt}}(N_s;N_\tau)$. For periodic BCs, indicated by the superscript p of a_3^p, they have a finite size behavior of the form

$$\beta^g_{\text{pt}}(N_s;N_\tau) = \beta^g_t(N_\tau) + a_3^p\left(\frac{N_\tau}{N_s}\right)^3 + \cdots, \tag{18}$$

which comes from the finite size scaling (FSS) analysis of the magnetic susceptibility in spin systems [18]. Relying on fits of this form estimates of $\beta^g_t(N_\tau)$ are given in [10].

Our data for $\beta^g_{\text{pt}}(N_s;4)$ are summarized in Table I. Within statistical errors the lattice size dependence of $\beta^g_{\text{pt}}(N_s;4)$ is almost negligible. A fit of our data with periodic BCs to (18) gives $\beta^g_t(4) = 5.692\,36(21)$ in agreement with the value 5.6925(2) reported in [10]. From now on we use $\beta^g_t(4) = 5.692\,36(21)$ as the infinite volume limit for periodic and disorder wall BCs.

Our estimates of $\beta^g_{\text{pt}}(N_s;6)$ are summarized in Table II. We took only few $N_\tau = 6$ data for periodic BCs, because they consume considerable CPU time and results exist already in the literature. Again they show almost no lattice size dependence. Fitting them to (18) gives $\beta^g_t(6) = 5.8926(18)$ in agreement with $\beta^g_t(6) = 5.8941(5)$ from [10]. In the following we use the latter, more accurate, $\beta^g_t(6)$ estimate of the literature.

The disorder wall BCs introduce an order N_s^2 disturbance, so that Eq. (18) becomes

$$\beta^g_{\text{pt}}(N_s;N_\tau) = \beta^g_t(N_\tau) + a_1^d\frac{N_\tau}{N_s} + a_2^d\left(\frac{N_\tau}{N_s}\right)^2 + a_3^d\left(\frac{N_\tau}{N_s}\right)^3 + \cdots, \tag{19}$$

where the superscripts d of the coefficients a_i^d indicate disorder wall BCs. The higher order corrections are needed to achieve consistency between the data and the fit.

In Fig. 1 we show the fit (19) to $\beta^g_t(4)$ and our pseudotransition values $\beta^g_{\text{pt}}(N_s;4)$ from simulations with the disorder wall BCs. The very precise infinite volume estimate $\beta^g_t(4)$ from simulations with periodic BCs is included in the disorder wall data to stabilize the fit at large volumes. For comparison the fit (18) for our $N_\tau = 4$ data from simulations with periodic BCs is also given. While finite size corrections are practically negligible for the simulations with periodic BCs, this is not the case for the disorder wall BCs. Q is the goodness of the fit (e.g., chapter 2.8 of [17]).

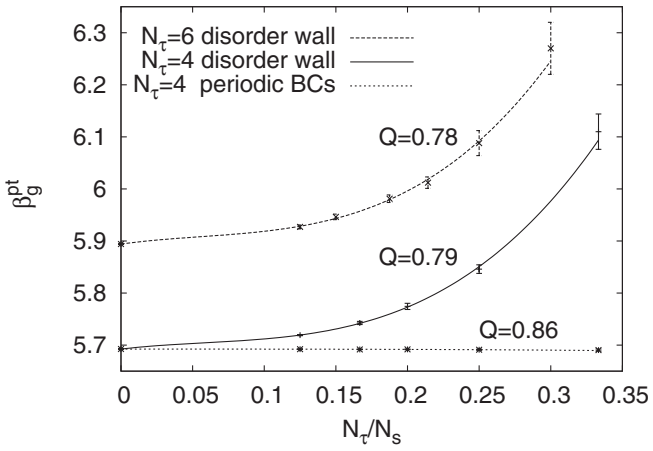

FIG. 1. Fits of pseudotransition coupling constant values and their infinite volume extrapolations.

We also include the fit (19) to $\beta^g_t(6)$ and our $\beta^g_{\text{pt}}(N_s;6)$ disorder wall data in Fig. 1. As expected both disorder wall curves show strong finite lattice size effects. This is not automatically of physical relevance. Important is whether universal corrections survive in the finite volume continuum limit. Here universal means that the corrections do not depend on the lattices used in the simulations, once these lattices are sufficiently large. In the following, we test this for $N_\tau = 4$ and $N_\tau = 6$ using the lambda scale (10) to calculate estimates in physical units. Although our β^g values used are rather small, they are in the previously reported [10] scaling region for Eq. (10), so that it is reasonable to expect universal behavior with moderate corrections.

The infinite volume T^c value (2), the lambda scale (10) and Eq. (9) give us the g^2 dependence of the lattice spacing a in units of fermi. Using the $N_\tau = 4$ fit to (19) of Fig. 1 together with Eqs. (1) and (6) allows to eliminate g^2 and we plot the resulting function $T^c(L_s)$ in Fig. 2. Repeating this procedure for our $N_\tau = 6$ fit to (19) gives, as is seen in Fig. 2, almost the same $T^c(L_s)$ dependence and thus provides evidence that our $N_\tau = 4$ and 6 results are already representative for the finite volume continuum limit. For a box of volume (10 fermi)^3 the pseudocritical temperature T^c is about 5% higher than the infinite volume estimate and this correction increases to about 17% for a (5 fermi)^3 box. For comparison we use the same procedure for analyzing the finite size dependence obtained by fitting the $N_\tau = 4$ and 6 data with periodic BCs (including and enforcing the $\beta^g_t(6) = 5.8941$ limit for $N_\tau = 6$) to Eq. (18). This gives the two lower curves of the figure, which fall almost on top of one another. In that case error bars are considerably smaller than for the disorder wall data.

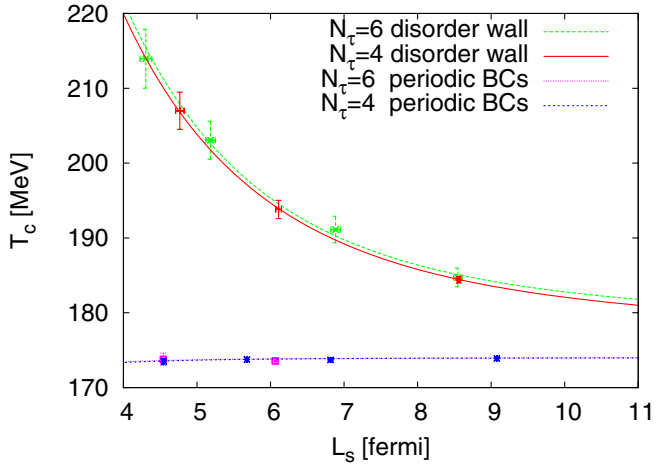

FIG. 2 (color online). Estimate of finite volume corrections to the deconfinement temperature, set at 174 MeV for an infinite volume.

For a first order phase transition the maxima of the Polyakov loop susceptibility have to scale with the system volume to reproduce the delta function like singularity of a first order transition. For $N_\tau = 4$ our $\chi_{\max}$ values are listed in Table III and for $N_\tau = 6$ in Table IV. Using $N_s \geq 16$ for $N_\tau = 4$ and $N_s \geq 20$ for $N_\tau = 6$ acceptable fits to the straight-line form

$$\chi_{\max} = d_1 + d_2(N_s/N_\tau)^3 \tag{20}$$

are obtained and shown together with their Q values in Fig. 3 (for $N_\tau = 6$ and periodic BCs only two data points are fitted, so that there is no Q value in that case). To enhance the scale for the disorder wall fits, they are displayed on the right ordinate. The leading coefficients obtained from fits for disorder wall data differ from those for the data with periodic BCs: $d_2^d = 0.011\,90(60)$ versus $d_2^p = 0.1436(37)$ for $N_\tau = 4$ and $d_2^d = 0.008\,43(95)$ versus $d_2^p = 0.0723(70)$ for $N_\tau = 6$. This is possible because the Polyakov loop maxima are not physical observables, but bare quantities.

Let us now consider the width of the transition. For a 4×16^3 lattice with disorder wall BCs the Polyakov loop susceptibility as a function of β^g is shown in Fig. 4. We use reweighting [17,19] to cover a range of β^g and define

TABLE III. Maxima of Polyakov loop susceptibility and width of the transition for lattices $4 \times N_s^3$.

	Periodic BCs		Disorder wall BCs	
N_s	$\chi_{\max}$	$\Delta\beta^g_{2/3}$	$\chi_{\max}$	$\Delta\beta^g_{2/3}$
12	3.585 (71)	0.0207 (11)	1.715 (27)	0.448 (18)
16	7.62 (16)	0.0103 (13)	1.879 (26)	0.0997 (21)
20	16.17 (67)	0.004 98 (68)	2.525 (84)	0.0440 (27)
24	28.6 (1.1)	0.002 77 (32)	3.58 (14)	0.0225 (16)
32	73.0 (2.0)	0.001 32 (16)	7.67 (39)	0.007 09 (61)

TABLE IV. Maxima of Polyakov loop susceptibility and width of the transition for lattices $6 \times N_s^3$.

	Periodic BCs		Disorder wall BCs	
N_s	$\chi_{\max}$	$\Delta\beta^g_{2/3}$	$\chi_{\max}$	$\Delta\beta^g_{2/3}$
18	2.47 (10)	0.0303 (21)	2.15 (20)	0.84 (04)
20	...	...	1.89 (10)	0.322 (25)
24	5.00 (27)	0.0162 (15)	1.90 (11)	0.140 (13)
28	...	...	2.18 (10)	0.0712 (69)
32	11.34 (55)	0.008 03 (66)	2.82 (16)	0.0422 (37)
40	...	...	4.21 (31)	0.0234 (17)
48	...	...	5.44 (99)	0.0123 (38)

$\Delta\beta^g_{2/3}$ as the width of a peak at $2/3$ of its height. On larger lattices, the data are less accurate than those shown in Fig. 4, but do still allow for the extraction of $\Delta\beta^g_{2/3}$. Within the same computer time the choice of the $2/3$ maximum definition of the width allows for more estimates than the conventional $1/2$ maximum definition, because appropriate β-patches are easier to obtain. In particular, using FSS information from our smaller lattices, we managed to focus simulations of our most expensive 6×48^3 lattice on just three β values, covering the maximum and the $2/3$ maximum values on the left and right flanks.

Our estimates of $\Delta\beta^g_{2/3}$ for $N_\tau = 4$ are listed in Table III and for $N_\tau = 6$ in Table IV. The data are fit to the form

$$\Delta\beta^g_{2/3} = c_1^p\left(\frac{N_\tau}{N_s}\right)^3 + c_2^p\left(\frac{N_\tau}{N_s}\right)^6 \tag{21}$$

for periodic BCs and to

$$\Delta\beta^g_{2/3} = c_1^d\left(\frac{N_\tau}{N_s}\right)^3 + c_2^d\left(\frac{N_\tau}{N_s}\right)^4 \tag{22}$$

for the disorder wall BCs. The first term reflects in both cases the delta function singularity of a first order phase transition, i.e., the width times the Polyakov loop maximum is supposed to approach a constant for $N_s \to \infty$. The

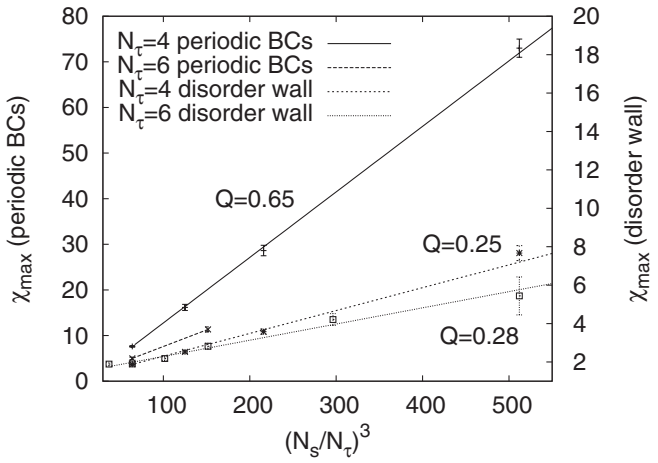

FIG. 3. Maxima of Polyakov loop susceptibility.

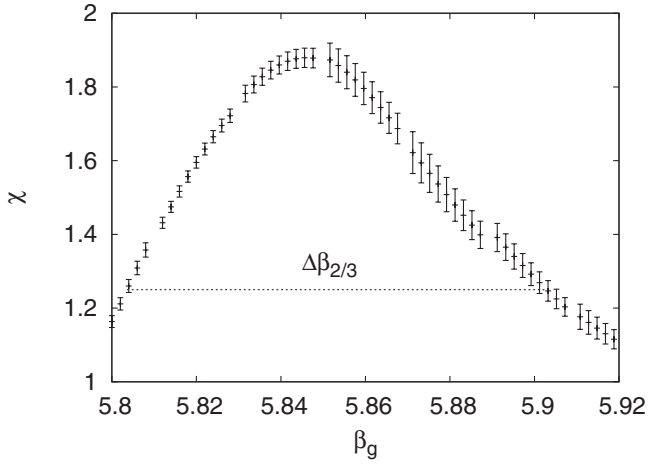

FIG. 4. The Polyakov loop susceptibility on a 4×16^3 lattice with disorder wall BCs.

leading order correction to that is $1/\text{Volume}$ for periodic BCs and $1/N_s$ for disorder wall BCs.

For $N_\tau = 4$ the final fits are shown in Fig. 5. From the disorder wall data we have omitted our smallest 4×12^3 lattice from the fit, because for it the width becomes so broad that it spoils Q (larger lattices than with periodic BCs are needed). The leading order coefficients are then $c_1^p = 1.17(55)$ and $c_1^d = 0.650(49)$. Both data sets can still be consistently fitted using the weighted average $c_1 = 0.654(49)$ of the leading order coefficients and 1-parameter fits for c_2 in (21) and (22). This ensures that the ratio of the widths becomes one in the infinite volume limit. In contrast to the Polyakov loop maxima, the width of the transition is a physical observable, which is to leading order in the volume independent of the BCs. These 1-parameter fits together with their Q values are what we show in Fig. 5.

The methodology for the corresponding $N_\tau = 6$ fits is the same. Using the data of Table IV we find the leading order coefficients $c_1^p = 1.27(11)$ and $c_1^d = 1.8(1.3)$, which average to $c_1 = 1.27(11)$. With these values consistent 1-parameter fits are obtained and together with their Q values depicted in Fig. 6. Note that the ordinate scale in this figure is more than 3 times larger than in Fig. 5. Nevertheless the extracted physical values have to be the same when scaling holds.

We want to plot the width in physical units of MeV versus the box size in fermi and follow a similar procedure as before for $T^c(L_s)$. For given $L_s(\beta^g)$ we define

$$\Delta T^c(L_s) = T(\beta^g_{\text{pt}} + \Delta\beta^g_{2/3}/2) - T(\beta^g_{\text{pt}} - \Delta\beta^g_{2/3}/2). \tag{23}$$

The dependence $\Delta T(L_s)$ is shown in Fig. 7. Compared to periodic BCs disorder wall BCs lead to a substantial broadening of the transition for the volumes considered: At $(10 \text{ fermi})^3$ by a factor of 4.3 and at $(5 \text{ fermi})^3$ by a factor of 5.5. For disorder wall BCs the width is slightly less than 1% of the (enhanced) transition temperature at $(10 \text{ fermi})^3$ and about 8% at $(5 \text{ fermi})^3$. Within the error bars, which are quite large for the widths, scaling again works well.

Simulations with disorder wall BCs have turned out to be far more CPU time consuming than those with periodic BCs. The decreased heights of our pseudotransition signals (i.e., the maxima of the Polyakov loop susceptibilities), their increased widths and the strong finite size effects are the underlying reasons. While the reweighting range [17,19] is about the same for simulations with periodic or disorder wall BCs on identically sized lattices, accurate disorder wall results require in general more patches, i.e., independent simulations at distinct β^g values. In addition the signal is worse due to the decreased heights of the peaks. Finally, extrapolations to infinite lattices, as needed for the finite volume continuum limit, are more demanding due to the strong and more sophisticated finite size corrections. This is helped by including infinite volume extrapolations from periodic lattices as disorder wall data points, which can be done because these extrapolations do not

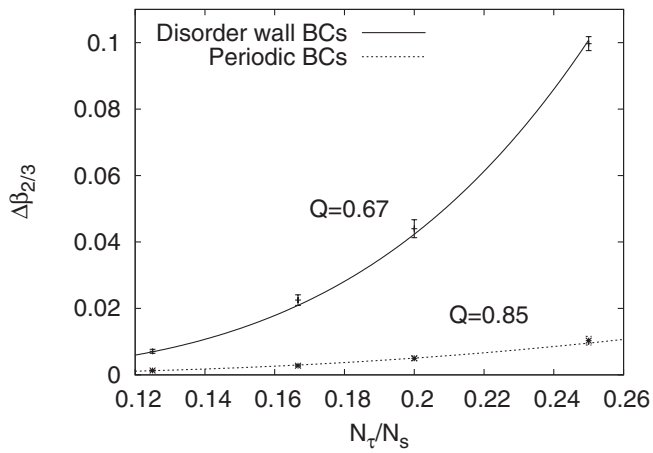

FIG. 5. Fits of the $N_\tau = 4$ width of the transition.

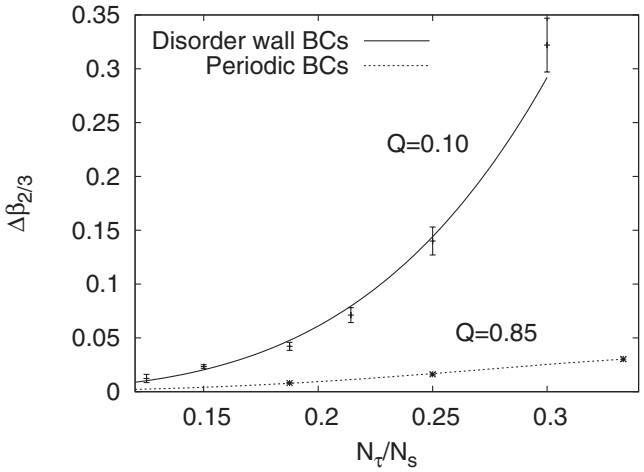

FIG. 6. Fits of the $N_\tau = 6$ width of the transition.

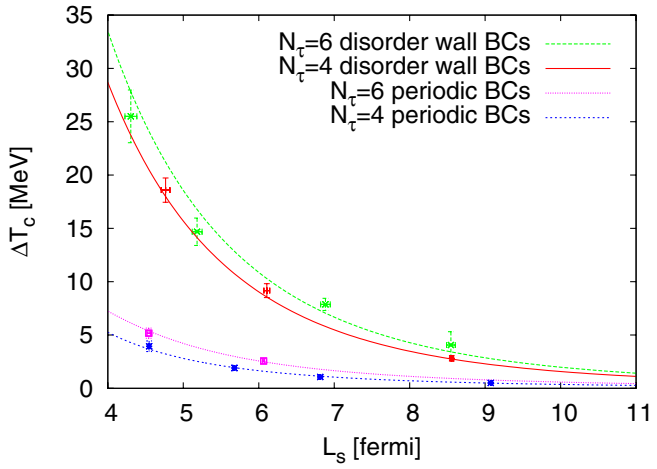

FIG. 7 (color online). Estimate of finite volume correction to the width of the deconfinement phase transition.

depend on the BCs. Still, data from our largest 6×48^3 lattice turn out to be essential to stabilize the $N_\tau = 6$ fits for large lattice sizes. Far smaller lattices are sufficient when periodic BCs are used.

IV. SUMMARY AND CONCLUSIONS

We considered LGT at high temperature in a volume, which is surrounded by a cold environment (outside volume). Balance of the Markov Chain Monte Carlo process allows to equilibrate both volumes despite the temperature jump at the boundary. In our first construction, called disorder wall, the spacelike lattice spacing changes when one crosses the boundary between inside and outside lattice. Our second construction, called confinement wall, aims to keep it constant. For a large temperature difference, say deconfinement temperature inside and room temperature outside, one is driven with at least one coupling constant of the outer lattice into the strong coupling region, if one demands that the inner lattice is in the scaling region of lattice sizes accessible by simulations. For the disorder wall this limit is particularly simple: $\beta = 0$ on the outer lattice, and we have performed MC simulations of pure SU(3) LGT for this case.

It is not *a priori* clear whether a boundary in the strong coupling region leads to corrections of scaling. So it is quite remarkable that our plots from $N_\tau = 4$ and $N_\tau = 6$ collapse within statistical errors to the same graphs (Figs. 2 and 7) when the scaling relation for the SU(3) Wilson action is used. There are no adjustable parameters at that point, as the scaling relation was previously determined [10]. For the volumes considered, we find a substantial rounding of the SU(3) transition with disorder BCs compared to periodic BCs: an increase of a pseudodeconfinement temperature between 5% and 20% and of the associated width by factors 4 to 6. In contrast to periodic BCs finite size corrections appear no longer negligible. The reason for this is that correlation lengths are proportional to L_τ and L_τ/L_s does not approach zero in a finite volume continuum limit. In magnitude the effects on pure SU(3) LGT are found to be competitive with other corrections, foremost the inclusion of quarks. However, because of the various limitations of our approximation of a cold exterior, our quantitative results cannot be taken too seriously at the moment. The main conclusion is that corrections due to cold boundaries deserve attention when the deconfined volume is only a few fermi in diameter.

Because of finite volume effects, the concept of a sharp transition can become blurred even when the effects of quarks, which convert the phase transition into a crossover [20], are not yet taken into account. Ultimately one may want to extend LGT studies of the deconfining transition with BCs reflecting the confined outside world to full QCD. Before doing so, additional experience can be gained from pure SU(3) LGT. A particularly attractive option would be to include an outside lattice, which is kept just slightly below the deconfinement temperature, using our confinement wall construction. That allows to keep both sides in their scaling regions and the spacelike lattice spacing constant. The obtained corrections may serve as lower bounds on corrections from a really cold outside volume. Further, one may want to extend the measurements to include gluonic energy density and entropy to estimate corrections to the equation of state.

ACKNOWLEDGMENTS

This work was in part supported by the U.S. Department of Energy under Contract No. DE-FG02-97ER41022.

[1] L. D. McLerran and B. Svetitsky, Phys. Lett. **98B**, 195 (1981); J. Kuti, J. Polónyi, and K. Szlachányi, Phys. Lett. **98B**, 199 (1981); J. Engels, F. Karsch, I. Montvay, and H. Satz, Phys. Lett. **101B**, 89 (1981).

[2] P. Petreczky, Nucl. Phys. B, Proc. Suppl. **140**, 78 (2005); E. Laermann and O. Philipsen, Annu. Rev. Nucl. Part. Sci. **53**, 163 (2003).

[3] We omit the adjective "quantum" in front of continuum limit from hereon. The classical continuum limit is not considered in our paper.

[4] H. J. Rothe, *Lattice Gauge Theories: An Introduction* (World Scientific, Singapore 2005), 3rd ed.

[5] Often the physical scale in pure gauge calculations is set by choosing a value of about 420 MeV for the string

tension $\sqrt{\sigma}$, which then leads via scaling to $T^c \approx 265$ MeV. However, in this paper we prefer to deal with a T^c value close to its physical QCD estimate, as one is ultimately interested in corrections to this value.

[6] For a review see, e.g., B. Muller and J. L. Nagle, Annu. Rev. Nucl. Part. Sci. **56**, 93 (2006).

[7] A. Bazavov, B. Berg, and A. Velytsky, Phys. Rev. D **74**, 014501 (2006).

[8] F. Brown, N. Christ, Y. Deng, M. Gao, and T. Woch, Phys. Rev. Lett. **61**, 2058 (1988); M. Fukugita, M. Okawa, and A. Ukawa, Phys. Rev. Lett. **63**, 1768 (1989); N. A. Alves, B. A. Berg, and S. Sanielevici, Phys. Rev. Lett. **64**, 3107 (1990).

[9] D. J. Gross and F. Wilczek, Phys. Rev. Lett. **30**, 1343 (1973); H. D. Politzer, Phys. Rev. Lett. **30**, 1346 (1973).

[10] G. Boyd, J. Engels, F. Karsch, E. Laermann, C. Legeland, M. Lütgemeier, and B. Petersson, Nucl. Phys. **B469**, 419 (1996).

[11] See Eq. (19) of [7].

[12] J. Kogut, R. Pearson, and J. Shigemitsu, Phys. Rev. Lett. **43**, 484 (1979); G. Münster and P. Weisz, Phys. Lett. **96B**, 119 (1980).

[13] G. Münster, Nucl. Phys. **B190**, 439 (1981); **B200**, 536(E) (1982).

[14] F. Karsch, Nucl. Phys. **B205**, 285 (1982).

[15] This follows from Eq. (1.4) of [14]. Note that in that equation $g_\sigma^2(a, \xi)/g_\tau^2(a, \xi) \to 1$ in the continuum limit due to Eq. (2.4) of [14].

[16] M. J. Teper, Phys. Rev. D **59**, 014512 (1998).

[17] B. A. Berg, *Markov Chain Monte Carlo Simulations and Their Statistical Analysis* (World Scientific, Singapore, 2004).

[18] K. Binder and D. Landau, Phys. Rev. B **30**, 1477 (1984); M. S. Challa, D. Landau, and K. Binder, Phys. Rev. B **34**, 1841 (1986).

[19] A. M. Ferrenberg and R. H. Swendsen, Phys. Rev. Lett. **61**, 2635 (1988); **63**, 1658(E) (1989), and references given therein.

[20] Y. Aoki, G. Endrődi, Z. Fodor, S. D. Katz, and K. K. Szabó, Nature (London) **443**, 675 (2006).